



**THE CONTRIBUTION OF RADIATION
PRESSURE TO THE STABILITY OF A
STANDARD THIN KEPLERIAN ACCRETION
DISK AROUND A NEUTRON STAR WITH
AXISYMMETRIC MAGNETIC FIELD DIPOLE**

By
HAFTAMU G/MARIAM

THIS THESIS IS SUBMITTED IN PARTIAL FULFILLMENT OF THE
REQUIREMENTS FOR THE DEGREE OF
MASTER OF SCIENCE IN PHYSICS(ASTRONOMY)

AT
ADDIS ABABA UNIVERSITY
ADDIS ABABA, ETHIOPIA
JUNE 2011

ADDIS ABABA UNIVERSITY
DEPARTMENT OF
PHYSICS

Advisor:

Dr.LEGESSE WOTRO

Examiners:

Prof.A.V GHOLAP

Prof.A.K CHAUBEY

ADDIS ABABA UNIVERSITY

Date: **JUNE 2011**

Author: **HAFTAMU G/MARIAM**

Title: **THE CONTRIBUTION OF RADIATION
PRESSURE TO THE STABILITY OF A
STANDARD THIN KEPLERIAN ACCRETION
DISK AROUND A NEUTRON STAR WITH
AXISYMMETRIC MAGNETIC FIELD DIPOLE**

Department: **Physics**

Degree: **M.Sc.** Convocation: **JUNE** Year: **2011**

Permission is herewith granted to Addis Ababa University to circulate and to have copied for non-commercial purposes, at its discretion, the above title upon the request of individuals or institutions.

Signature of Author

THE AUTHOR RESERVES OTHER PUBLICATION RIGHTS, AND NEITHER THE THESIS NOR EXTENSIVE EXTRACTS FROM IT MAY BE PRINTED OR OTHERWISE REPRODUCED WITHOUT THE AUTHOR'S WRITTEN PERMISSION.

THE AUTHOR ATTESTS THAT PERMISSION HAS BEEN OBTAINED FOR THE USE OF ANY COPYRIGHTED MATERIAL APPEARING IN THIS THESIS (OTHER THAN BRIEF EXCERPTS REQUIRING ONLY PROPER ACKNOWLEDGEMENT IN SCHOLARLY WRITING) AND THAT ALL SUCH USE IS CLEARLY ACKNOWLEDGED.

Table of Contents

Table of Contents	iv
List of Figures	v
Abstract	vi
Acknowledgements	vii
Introduction	1
1 The Physics of Neutron Stars	4
1.1 Neutron Star Formation	4
1.2 The Structure of Neutron Star	5
1.3 Accretion In Neutron Star	7
1.3.1 Accretion Disc	8
1.3.2 Accretion Column	9
1.4 X-ray Binaries	9
2 Basic Equations for thin Accretion Disks (Non-Relativistic theory)	12
2.1 Introduction	12
2.2 Equation Of State	13
2.3 Mass Conservation	14
2.4 Angular Momentum Conservation	14
2.5 Radial Momentum Conservation	16
2.6 Energy Conservation	16
2.7 Equations for the vertical structure	17
3 Steady keplerian Disks and Standard Disks	19
3.1 Steady keplerian Disks	19
3.1.1 Radial structure Equations	19
3.1.2 Vertical structure Equations	20
3.2 Standard Disks	21
3.2.1 Viscosity	21
3.2.2 vertical structure	22

3.2.3	Radial structure	24
4	Stability Analysis Of Thin Accretion Disks	29
4.1	Dynamic Equation	29
4.2	Thermal Equation	30
4.3	Linearization	32
4.4	Estimating The Radius of Instability Of The Inner Region Of The Disk .	36
5	conclusion	40
	Appendix	41
	References	46

List of Figures

1.1	neutron star structure	6
1.2	A binary system with the secondary star filling the roche lobe and transferring mass through L_1 into the lobe of the compact primary.	8
1.3	Binary system of a compact object and a companion star. Accreting gas forms a disk around the compact object.	10
1.4	a LMXB system and its typical length length scales.	11
4.1	Instability growth rate when radiation pressure dominates ($\beta_o > \frac{3}{5}$) as a function of wavelength Λ . Broken lines denote traveling waves, continuous lines denotes standing waves. Upper branches correspond to thermal instabilities and lower branches to dynamic instabilities.(from[3]).	35

Abstract

In this thesis, we have studied the dynamic properties of an accretion disk formed from the inflow of plasma from a blotted out companion star. The disk extends from an inner radius of $\sim 10^6 m$ (R_A Alfeven radius) to $100R_A$ (see figure 1.4). We have divided the disk into three regions: an outer region dominated by gas pressure and free-free opacity, a middle region dominated by gas pressure and electron scattering, and an inner region dominated by radiation pressure and electron scattering. We have also derived the radiation pressures and gas pressure in the inner region of the disk as a function of "r" using radial dependence of the central temperature and the density. The latter was obtained using the basic equations for thin accretion in non-relativistic case . Analyses of the instability of the disk is made between R_A and $10R_A$ ($R_A < r < 10R_A$) based on the instability condition ($\beta_o > 3/5$). This is occurred at high temperature, at which the opacity is dominated by electron scattering and radiation pressure is strong.

Acknowledgements

First I would like to express my deepest gratitude to my advisor Dr. Legesse Wotro Kebede for his unreserved assistance, constructive guidance, valuable suggestions and the kind of hospitality he has given me during the course of my thesis. His scientific excitement, integral view on the research and overly enthusiasm, has made a deep impression on me. I am also thankful to the Astrophysics group (G/her, Melkamshet, Ossman and Abi) for their contribution in strengthening the group and the completion of this paper.

My special thank to my Father and Tsige.T, with out their push and support,none of this would have been possible. At last, I am also grateful to all of my family and friends, for various useful comments and advise.

Introduction

The stability of geometrically thin accretion disks has been studied extensively after the construction of the standard model [1]. It has been found that the disk is thermally and viscously unstable if it is optically thick and radiation pressure dominated [2-4]. There is also a possible mode of pulsational stability. In this case, one looks for instabilities in which oscillations on the orbital time scale grow in amplitude because of the effects of viscosity [5]. Blumenthal, Yang and Lin generalized functional form for the viscosity and the opacity. They used their model to interpret successfully the quasi-periodic oscillation observed in dwarf novae. Okuda examined a radial oscillation model of accretion disks for quasi-periodic light variations in cataclysmic variables [7]. Chen and Tamm pointed out that the galactic black hole candidates may be due to the pulsational stability [8]. If the geometrically thin disk is optically thin, it has been found also that it is viscously stable but thermally unstable [9]. Those instabilities are believed to be relevant to some light variation observed in many systems such as cataclysmic variables, X-ray binaries, and active galactic nuclei. For example, the thermal instability may account for the periodic outburst of dwarf nova [10], and the inertial acoustic instability may explain the observed QPO phenomena in Galactic black hole candidates [8].

Since the standard thin disk model was constructed in the early 1970 [1], the stability of disk has become an important area in the accretion disk theory in stabilities of accretion disks permitted to explain the observed phenomena of variability and luminosity of various astronomical objects. such as proto- planetary nebulae of dwarf novae, X-ray binaries, active galactic nuclei and quasars.

Lightman and Eardley found that the inner most region of an accretion disk, the disk flow would be viscously unstable if the radiation pressure dominates [4]. subsequently, Shakura and Sunyaev showed that these inner regions of the disk may also be thermally unstable [2]. kato considered the evolution of infinitesimal perturbations of all three components of the fluid velocity as well as T and S .He found that the disk had pulsational instability in addition to viscous and thermal instabilities[11]. Blumenthal generalized katos analysis by considering the pulsation stability criterion for a thin disk model with different ratios of gas pressure to radiation pressure, arbitrary values of α , a general functional form for the viscosity ν and other opacity κ [6]. They used their model to interpret successfully the quasi period oscillations observed in draw novae. There are two kinds instabilities in an isothermal disk when α is larger than a critical value [12]. one is the pulsational insatiability and the other is sonic-point instability, which is local to the sonic point . The sonic point is related to the topology of the sonic point [13]. Chen and Tamm performed a numerical study on the structure and stability of accretion disks, taking in to consideration radial viscosity. They showed that the radial viscosity has stabilizing influence on the viscous mode [14]. Wu Xuebing and Yu wnfei considered the influence of radial viscosity on the Stability of a polytropic and an isothermal magnetized accretion disk, respectively [15,16].

Magnetic fields can play an important role in accretion disks. For example ,magnetic fields have been invoked as a source of coronal heating [17],wind production [18] and highly polarized radiation [19]. An accretion disk around a weakly magnetized neutron star forms an s- shaped sequences on the M-S plane ,this model sequence is named ” *slim*” disks [20]. Balbus and Hawley showed that accretion disks are dynamically unstable to an axisymmetric shear instability whenever a weak vertical magnetic field is present [21]. Wu xuebing examined the pulsational instability of isothermal accretion disk with viscosity and magnetic fields [15].

In this thesis, our aim is to determine the radial location of instability in the inner

region of the accretion disk around a magnetized star. Therefore, in the spirit of Shakura and Sunyaev [1,3] we divide the disk into three regions, an outer region dominated by gas pressure and free-free opacity, a middle region dominated by gas pressure and electron scattering, and an inner region dominated by radiation pressure and electron scattering.

The structure of this thesis is as follows, The first chapter is devoted to the discussion of the physics of a neutron star, in which the formation, structure, internal composition is described. In chapter two the basic equations of thin accretion disks for non-relativistic case, such as the equation of state, conservation of mass, angular and radial momentum, energy and equations for the vertical structure are briefly discussed. Steady Keplerian disks and standard disks are fully dealt with in chapter three. The stability analysis of the thin accretion disks and estimating of the radius of instability of the inner region in which radiation pressure dominated region is given in chapter four. Finally we made a conclusion.

Chapter 1

The Physics of Neutron Stars

Neutron stars are some of the densest manifestation of massive objects in the universe. In the following sections we will describe the formation , structure, internal composition of neutron star. Observations such as mass transfer (accretion) in neutron stars is also included with the discussion of the limit on the steady accretion rate , $\dot{M}(gs^{-1})$, which is the Eddington limit,the reason for mass transfer as a Roche lobe overflow in our case, formation of accretion disc and accretion column.

1.1 Neutron Star Formation

Compact objects such as neutron stars, white dwarfs and ultimately black holes represents the final states of stellar evolution[22]. When very massive stars (up to $25M_{\odot}$) ,where M_{\odot} is solar mass,die, after they have finished their nuclear fuel, they spew their outer layers into space in a violent explosion called supernova.The cores of such stars remain as neutron stars. So, a neutron star is a type of remnant that can result from the core collapse of a massive star during supernova event[23]. A supernova occurs when the iron core of a giant star collapses to the density of the nucleus. At such events high densities,protons and electrons fuse together to form neutrons[24]. Hence the name 'neutron star'. Neutron stars are very hot and are supported against further collapse because of degenerate neutron pressure resulting from Pauli exclusion principle. This principle states that no two neutrons can occupy the same quantum state simultaneously.

In general, compact stars with mass $< 1.4M_{\odot}$ are white dwarfs. On the other hand, a neutron star is about 20 km in diameter and has mass of about $1.4M_{\odot}$. This means that a neutron star is so dense that one teaspoonful of neutron star matter would weight a billion tons! The result is a surface gravitational field strength about 2×10^{11} times that of the earth. A neutron star can also have magnetic fields a million times strongest magnetic field produced on the earth[25]. As the core of a massive star is compressed during supernova, and collapse into a neutron star it retains most of its angular momentum. Since it has only a tiny fraction of its parents radius (its moment of inertia is reduced sharply) so that a neutron star is formed with very high rotation speed. It gradually slows down due to mostly gravitational radiation initially and then electromagnetic radiation. The number of neutron stars in the Galaxy has been estimated to be of the order 10^9 [26]. The number of observed neutron stars is much lower, about 800 are observed as radio pulsar[27], and about 150 as X-ray binaries. The population of neutron stars is concentrated along the disc of the milkway although the spread perpendicular to the disc is fairly large. The reason for this spread is that neutron stars born with high speeds (400 km/s) as a result of an imparted momentum kick from an asymmetry during the supernova explosion.

1.2 The Structure of Neutron Star

Current understanding of the structure of neutron stars is defined by existing mathematical models, but it might be possible to infer through studies of neutron-star oscillations. Similar to asteroseismology for ordinary stars, the inner structure might be derived by analyzing observed frequency spectra of stellar oscillations. On the basis of current models, the matter at the surface of a neutron star is composed of ordinary atomic nuclei crushed into a solid lattice with a sea of electrons flowing through the gaps between them. It is possible that the nuclei at the surface are iron, due to irons high binding energy per nucleon. It is also possible that heavy element cores, such as iron, simply drown beneath

the surface, leaving only light nuclei like helium and hydrogen cores. If the surface temperature exceeds 10^6 kelvins (as in the case of a young pulsar), the surface should be fluid instead of the solid phase observed in cooler neutron stars (temperature $< 10^6$ kelvins). The atmosphere of the star is roughly one meter thick, and its dynamic is fully controlled by the star's magnetic field. Below the atmosphere one encounters a solid “*crust*“. This crust is extremely hard and very smooth (with maximum surface irregularities of 5 mm, because of the extreme gravitational field). Proceeding inward, one encounters nuclei with ever increasing numbers of neutrons; such nuclei would decay quickly on Earth, but are kept stable by tremendous pressures. Proceeding deeper, one comes to a point called neutron drip where free neutrons leak out of nuclei. In this region, there are nuclei, free electrons, and free neutrons. The nuclei become smaller and smaller until the core is reached, by definition the point where they disappear altogether. The exact nature of the superdense matter in the core is still not well understood. While this theoretical substance is referred to as neutronium in science fiction and popular literature, the term “*neutronium*” is rarely used in scientific publications, due to ambiguity over its meaning. The term neutron-degenerate matter is sometimes used, though not universally as the term incorporates assumptions about the nature of neutron star core material.

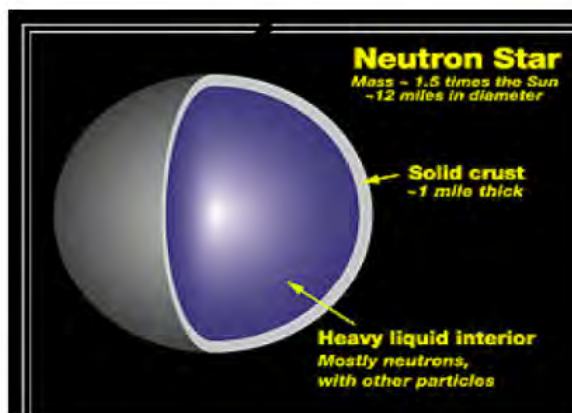


Figure 1.1: neutron star structure

Neutron star core material could be a super fluid mixture of neutrons with a

few protons and electrons, or it could incorporate high-energy particles like pions and kaons in addition to neutrons, or it could be composed of strange matter incorporating quarks heavier than up and down quarks, or it could be quark matter not bound into hadrons. (A compact star composed entirely of strange matter would be called a strange star.) However, so far, observations have neither indicated nor ruled out such exotic states of matter.

1.3 Accretion In Neutron Star

By accretion, we mean the accumulation of diffuse gas or matter onto some object under the influence of gravity. The extraction of gravitational potential energy from material which accrete onto a gravitating body is known to be the principal source of power in several types of close binary systems (as will be treated in the following section), and is widely believed to provide the power supply in active galactic nuclei, and quasars. Thus, the new role for gravity arises because accretion on to compact objects is natural and powerful mechanism for the production of high energy radiation. Some simple order of magnitude estimate will show how this works. For a body of mass M_o and radius R_o the gravitational potential energy released by the accretion of a mass M on its surface is $\Delta E = \frac{GM_o\Delta M}{R_o}$. If the accreting body is neutron star with radius $R_0 = 10km$ and $M_0 = M$, then the yield ΔE is about 1.3×10^{20} erg per accreted gram. This radiation is expected to be released mainly in the form of electromagnetic radiation [28]. For comparison, we refer to the energy released to the Hydrogen burning in which Hydrogen atoms fuse to produce Helium atoms: $\Delta E_{nuc} = 6 \times 10^8 \text{ergg}^{-1}$. Therefore, we can see that $\Delta E_{nuc} \ll \Delta E$. At high luminosity, the accretion rate may itself be controlled by an outward momentum transferred by scattering and absorption. It might seem as though we could generate arbitrarily large luminosities by allowing material to fall at a sufficiently great rate onto a star. However, there is a limit to this luminosity, since if the luminosity is too great, radiation pressure will blow away the in falling matter. This limiting luminosity, which is

known as the Eddington luminosity, is found by balancing inward force of gravity against the outward pressure of the radiation [29].

1.3.1 Accretion Disc

The initial trajectory of matter issued from L_1 would be an elliptical orbit lying in the binary plane. The presence of the secondary causes the orbit to precess slowly. The stream will therefore intersect itself, resulting in dissipation of energy. However since the angular momentum is conserved, the gas will tend to the orbit of lowest energy for a given angular momentum, i.e. a circular orbit. In most cases the total mass of gas in the disk is so small that we can neglect the self-gravity of the disk. The circular orbit is

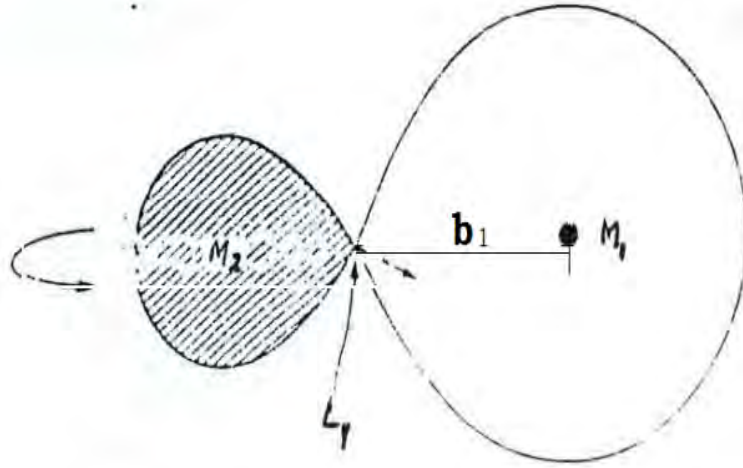


Figure 1.2: A binary system with the secondary star filling the roche lobe and transferring mass through L_1 into the lobe of the compact primary.

then Keplerian with angular velocity $\Omega_R = \left(\frac{GM_1}{R_{circ}^3}\right)^{\frac{1}{2}}$. The radius of this circular orbit is called the circularization radius R_{circ} . It is determined from the relation $\left(\frac{GM_1}{R_{circ}^3}\right)^{\frac{1}{2}} = b_1^2 \omega$. Then $\frac{R_{circ}}{a} = (1 + q)[0.5 - 0.227 \log q]^4$, where "a" is the binary separation and $q = \frac{M_2}{M_1}$. Within the ring of radius R_{circ} , there will be dissipative processes, such as collisions, shocks, and viscous dissipation. These will convert some of the energy of the ordered bulk orbital motion into internal energy (heat). Eventually some of this energy is radiated and

therefore lost from the gas. As a result the gas has to sink deeper into the gravitational potential of the primary, orbiting it more closely. This in turn will make it lose angular momentum. So most of the gas will spiral inwards towards the primary through a series of approximately circular orbits. The angular momentum is transferred outwards through the disk by viscous torques. The outer parts of the ring will gain angular momentum and will spiral outwards. The original ring of matter at $R = R_{circ}$ will spread to both smaller and larger radii by this process, to form an accretion disk [30].

1.3.2 Accretion Column

Column accretion occurs when the accreting star possess a magnetic field strong enough to disrupt the inner regions of the disc channeling the accretion flow in such a way that nearly resembles free-fall on the magnetic polar caps.

1.4 X-ray Binaries

X-ray binaries belong to the system in which a compact object and a stellar companion orbit each other at a distance small enough to enable mass transfer from the companion star(secondary or donor) onto the compact object(primary or accretor) [31]. X-ray binaries containing a neutron star or a black hole can be divided into two classes based on the mass of the companion star: high mass X-ray binaries(HMXBs) having a stellar companion usually more massive than $10M_{\odot}$, and low mass X-ray binaries(LMXBs)having a stellar companion with a mass around $1M_{\odot}$ or less. In HMXBs mass transfer is caused by the stellar wind of the compact star , while in LMXBs mass is accreted by Roche lobe overflow from a low mass star to a neutron star(see below). Neutron stars in X-ray binaries are relatively young and theoretically estimated to have a strong magnetic field of the strength $10^{12} - 10^{13}G$ [32]. The Roche model makes use of gravitational equipotential surfaces. The equipotential surface through L_1 , the point where the gravitational forces of the companion and the compact object and the centrifugal force cancel, consists

of two lobes called the Roche lobes. When, due to its evolutionary phase of expansion, the companion fills its Roche lobe, matter will stream through L_1 to the compact object. This process is called Roche lobe overflow. Because both binary components orbit each other, and because of conservation of angular momentum, the transferred mass is not able to fall straight to the compact object and therefore forms a disk from which matter spirals inwards following the magnetic field lines. The gas in the accretion disk also transports angular momentum outwards by friction and viscosity. The flow from the companion star causes a "hot spot" at the point where it reaches the accretion disk. Due to the large amounts of gravitational energy (up to several 10^{38} erg/s) that are released by this accretion, matter is heated up to $\sim 10^7 \text{ K}$ which is high enough for thermal X-ray emission. X-ray binaries are the brightest X-ray sources in the sky (after the sun). In the case of neutron stars, the X-ray emission originates from both the accretion disk and the neutron star surface, whereas in black holes the X-ray emission only comes from the accretion disk because black holes do not have a solid surface.

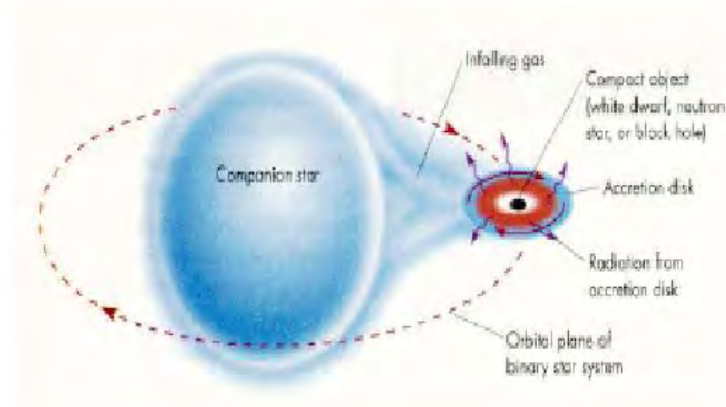


Figure 1.3: Binary system of a compact object and a companion star. Accreting gas forms a disk around the compact object.

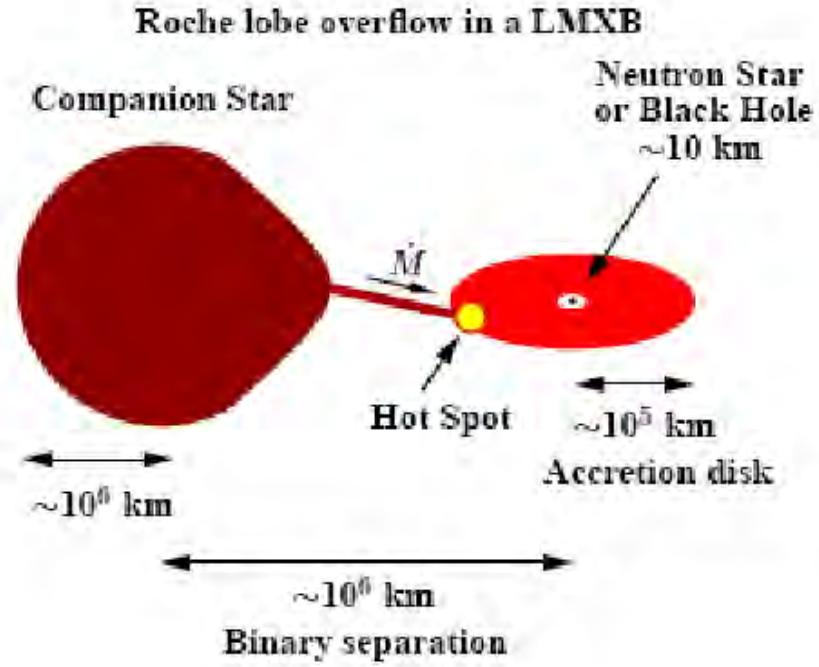


Figure 1.4: a LMXB system and its typical length length scales.

Chapter 2

Basic Equations for thin Accretion Disks (Non-Relativistic theory)

2.1 Introduction

Under many circumstances the matter accreting on to a compact object will have significant angular momentum and will therefore form a disk. The gas elements in the disk lose angular momentum, due to friction between adjacent layers. The released gravitational energy either increases the kinetic energy of rotation or converted into thermal energy which is radiated from the disk surface. Thus, viscosity converts gravitational potential energy in an efficient manner into radiation. The behavior of rotating gas masses and the formation of disks have been studied already long ago- before the interest in accretion driven x-ray sources- in connection with the evolution of the early solar nebula. An important example is Von Weizsackers paper [33], entitled the rotation of cosmic gas masses, in which he derived some of the basic equations which will be important in this section. He suggested also that turbulent viscosity should be the dominant dissipation process. Later, in 1952, this problem was taken up again by Lust [34].

Fairly direct evidence for the presence of disk accretion is available in many cataclysmic variables. We have also seen that there is good evidence for disk accretion in x-ray busters.

In this chapter we set up the basic equations which deliver the structure of thin accretion disks. We use non relativistic hydrodynamics. In view of the uncertainties as

to the nature and magnitude of the viscosity, for the stability analysis of disk models it is necessary to keep the time dependence in the equations.

Notations and the basic equations of the hydrodynamics are summarized in the Appendix.

2.2 Equation Of State

Since we are concerned with fully ionized disk plasmas, the pressure is the sum of the gas and radiation pressures,

$$P = P_g + P_r = \frac{k}{\mu m_H} \rho T + \frac{a}{3} T^4. \quad (2.2.1)$$

The internal specific energy is

$$\varepsilon = c_\nu T + \frac{aT^4}{\rho}$$

Let $\gamma = c_p/c_\nu$, $P_g = \beta P$. Using $c_p = c_\nu + k/\mu m_H$ We get

$$\varepsilon = \frac{3P_r}{\rho} + c_\nu \frac{P_g}{\rho(c_p - c_\nu)} = \frac{P}{\rho} \left[\frac{\beta}{\gamma - 1 + 3(1 - \beta)} \right]$$

Thus

$$\varepsilon = A \frac{P}{\rho}, A = \frac{\beta}{\gamma - 1} + 3(1 - \beta). \quad (2.2.2)$$

To describe the axisymmetric structure of an accretion disk, we employ cylindrical coordinates (r, φ, z) with the z -axis chosen as the axis of rotation ($z=0$ is the central plane of the disk). The mean velocity field v is a small perturbation of the keplerian circular motion $(0, (GM/r)^{1/2}, 0)$.

2.3 Mass Conservation

The continuity equation is (dropping the φ -derivatives)

$$\partial_t \varrho + \frac{1}{r} \partial_r (r \varrho v_r) + \partial_z (\varrho v_z) = 0. \quad (2.3.1)$$

Let us integrate this equation over the z -direction

$$\partial_t \int \varrho dz + \frac{1}{r} \partial_r \left(\int r \varrho v_r dz \right) = 0. \quad (2.3.2)$$

A useful variable is the surface density

$$S(r, t) = \int \varrho dz \quad (2.3.3)$$

For thin disks (height much smaller than radial variable), we can neglect the vertical variation of v_r in the second integral of Eq.(2.3.2) and thus obtain

$$\partial_t S + \frac{1}{r} \partial_r (r S v_r) = 0 \quad (2.3.4)$$

or, introducing the accretion rate

$$\dot{M}(r, t) = -2\pi r v_r S \quad (2.3.5)$$

We also have

$$\partial_r S = \frac{1}{2\pi r} \partial_r \dot{M} \quad (2.3.6)$$

Equation (2.3.4) can also be obtained by applying the mass conservation to an annulus of gas with inner radius r and with radial extent δr . similarly, the consequences of energy and angular momentum conservation can be deduced.

2.4 Angular Momentum Conservation

Next we consider the φ -component of the momentum equation (A.11) of the appendix . we find

$$\varrho \left(D_t \nu_\varphi + \frac{\nu_r \nu_\varphi}{r} \right) = \frac{1}{r} \partial_r (r t_{\varphi r}) + \partial_z t_{\varphi z} + \frac{1}{r} t_{r\varphi}. \quad (2.4.1)$$

If we multiply this equation with r and use

$$D_t = \partial_t + \nu_r \partial_r + \nu_z \partial_z. \quad (2.4.2)$$

For φ -independent functions, we obtain

$$\varrho D_t (r \nu_\varphi) = \frac{1}{r} \partial_r (r^2 t_{r\varphi}) + \partial_z (r t_{z\varphi}). \quad (2.4.3)$$

Now we multiply the continuity equation (2.3.1) with $r \nu_\varphi$ and add the resulting equation to Eq.(2.4.3). This gives

$$\partial_t (\varrho r \nu_\varphi) + \frac{1}{r} \partial_r (r \nu_r \varrho r \nu_\varphi) + \partial_z (\nu_z \varrho r \nu_\varphi) = \frac{1}{r} \partial_r (r^2 t_{r\varphi}) + \partial_z (r t_{z\varphi}). \quad (2.4.4)$$

Integrating over z gives the exact equation

$$\partial_t \int \varrho r \nu_\varphi dz + \frac{1}{r} \partial_r \int \nu_r \varrho r^2 \nu_\varphi dz = \frac{1}{r} \partial_r (W_{r\varphi} r^2). \quad (2.4.5)$$

Where

$$W_{r\varphi} = \int t_{r\varphi} dz. \quad (2.4.6)$$

Equation(2.4.5) follows also from angular momentum conservation.

For thin disks Eq.(2.4.5) is approximately

$$\partial_t (S r \nu_\varphi) + \frac{1}{r} \partial_r (\nu_r S r^2 \nu_\varphi) = \frac{1}{r} \partial_r (r^2 W_{r\varphi}) \quad (2.4.7)$$

With the aid of Eq.(2.3.4) this can also be written as

$$S [\partial_t (r \nu_\varphi) + \nu_r \partial_r (r \nu_\varphi)] = \frac{1}{r} \partial_r (r^2 W_{r\varphi}). \quad (2.4.8)$$

Note that $r \nu_\varphi$ is the specific angular momentum. Eq.(2.4.4) has the form of a conservation equation for angular momentum.

The component $t_{r\varphi}$ has the form

$$t_{r\varphi} = \eta r \partial_r \left(\frac{\nu_\varphi}{r} \right), \quad (2.4.9)$$

Where η the dynamic viscosity coefficient

2.5 Radial Momentum Conservation

The radial component of the momentum equation is

$$\varrho \left(D_t \nu_r - \frac{\nu_\varphi^2}{r} \right) = -\varrho \partial_r \phi - \partial_r P + \frac{1}{r} \partial_r (r t_{rr}) + \partial_z t_{rz} - \frac{1}{r} t_{\varphi\varphi}. \quad (2.5.1)$$

Except for $t_{r\varphi}$, all viscous stresses can be neglected. Neglecting also the z-component of ν , we have to sufficient accuracy

$$\varrho (\partial_t \nu_r + \nu_r \partial_r \nu_r) = \varrho \left(\frac{\nu_\varphi^2}{r} - \partial_r \phi \right) - \partial_r P \quad (2.5.2)$$

and after integrating over z

$$S (\partial_t \nu_r + \nu_r \partial_r \nu_r) = S \left(\frac{\nu_\varphi^2}{r} - \frac{GM}{r^2} \right) - \partial_r W, \quad (2.5.3)$$

Where

$$W = \int P dz. \quad (2.5.4)$$

2.6 Energy Conservation

Our starting point is Eq.(A.25) of the Appendix. The dominant part of $\mathfrak{t} \cdot \nu$ is the radial component of magnitude $t_{r\varphi} \nu_\varphi$ and thus

$$\text{div}(\mathfrak{t} \cdot \nu) \simeq \frac{1}{r} \partial_r (r t_{r\varphi} \nu_\varphi).$$

Ignoring again the z- component of the velocity and in addition the radial component of the energy flux vector, we have

$$\varrho (\partial_t + \nu_r \partial_r) \left(\frac{1}{2} \nu_r^2 + \frac{1}{2} \nu_\varphi^2 + h + \phi \right) = \partial_t P + \frac{1}{r} (r t_{r\varphi} \nu_\varphi) - \partial_z F, \quad (2.6.1)$$

Where F is the vertical energy flux density ($F = q_z$). we use Eq.(2.2.2) and integrate over z, In the thin disk approximation we obtain

$$S (\partial_t + \nu_r \partial_r) \left[\frac{1}{2} \nu_r^2 + \frac{1}{2} \nu_\varphi^2 + (A+1) \frac{W}{S} + \phi \right] = \partial_t W + \frac{1}{r} \partial_r (r W_{r\varphi} \nu_\varphi) - Q^-, \quad (2.6.2)$$

Where Q^- is the energy flux per unit area emitted at the disk surface: $Q^- = 2F$ (surface).

We also note that the dissipation function Eq.(A.20) is

$$\Upsilon = 2t_{r\varphi}\theta_{r\varphi} = t_{r\varphi}r\partial_r\left(\frac{\nu_\varphi}{r}\right) \quad (2.6.3)$$

and thus

$$Q^+ = \int \Upsilon dz = W_{r\varphi}r\partial_r\left(\frac{\nu_\varphi}{r}\right) \quad (2.6.4)$$

is the energy produced per unit area.

2.7 Equations for the vertical structure

The z-component of the momentum equation contains only the small components of the viscosity tensor. Ignoring these we have

$$\varrho D_t \nu_z = -\varrho \partial_z \phi - \partial_z P. \quad (2.7.1)$$

we assume that motions in the z-direction are subsonic. then, as we show later, the left hand side is of order $(z/r)^2$. Neglecting such terms for thin disks, we obtain

$$\partial_z P = -\varrho \frac{GM}{r^2} \frac{z}{r}, \quad (2.7.2)$$

i.e ,we have hydrostatic equilibrium in the z-direction. (this is not surprising since there is no net motion in the vertical direction) From Eq.(2.7.2) we see that the disk half-thickness z_0 is roughly given by $z_0/r \approx c_s/\nu_\varphi$, where c_s is the speed of sound . The thin disk requirement thus says that the circular flow velocity is highly supersonic. This poses restrictions on the disk interior temperature, which are only satisfied if the gas cools sufficiently fast.

We also see that the time it takes for a sound wave to travel the distance z_0 is $z_0/c_s \sim \Omega^{-1}$,where Ω is the keplerian angular velocity.

Usually it is assumed that the energy dissipated in to heat is radiated on the spot in the vertical direction. Then we have [(see Eq.(2.6.3)]

$$\partial_z F = \Upsilon = t_{r\varphi} r \partial_r \left(\frac{\nu_\varphi}{r} \right). \quad (2.7.3)$$

In addition, we need an energy transport equation in the z - direction , which will be written down later.

Some of the equations are simplified if one approximates by the circular keplerian velocity,

$$\nu_\varphi \simeq \Omega r, \quad \text{where} \quad \Omega = \left(\frac{GM}{r^3} \right)^{1/2}. \quad (2.7.4)$$

Then $\partial_t \nu_\varphi = 0$ and we obtain from Eq.(2.4.8)

$$\frac{\dot{M}\Omega r}{2} = -2\pi \partial_r (W_{r\varphi} r^2) \quad (2.7.5)$$

with

$$W_{r\varphi} = r \frac{d\Omega}{dr} \int \eta dz \quad (2.7.6)$$

and thus

$$\dot{M}\Omega r^2 + 2\pi r^3 \frac{d\Omega}{dr} \int \eta dz = \dot{I}, \quad (2.7.7)$$

Where \dot{I} is independent of r . The keplerian approximation follows from Eq.(2.5.3) if inertia and pressure gradient terms are neglected. Corrections are of order $(z_o/r)^2$ (see later).

For Eq.(2.7.3) we find

$$\partial_z F = \frac{9}{4} \eta \frac{GM}{r^3} \quad (2.7.8)$$

and Eq.(2.6.4) becomes

$$Q^+ = \frac{9}{4} \eta \frac{GM}{r^3} \int \eta dz. \quad (2.7.9)$$

Chapter 3

Steady keplerian Disks and Standard Disks

3.1 Steady keplerian Disks

We summarize first the basic equations for steady disks in the keplerian approximation $\Omega = (GM/r^3)^{1/2}$.

3.1.1 Radial structure Equations

The continuity equation gives

$$\dot{M} = -2\pi r S \nu_r = \text{const.} \quad (3.1.1)$$

The angular momentum conservation Eq.(2.7.5) implies

$$\dot{M} r^2 \Omega = -2\pi r^2 W_{r\varphi} + \dot{I}. \quad (3.1.2)$$

Here the constant \dot{I} is the net inward flux of angular momentum, whose value is usually assumed to be of order $\dot{M} r_o^2 \Omega(r_o)$ (r_o is the inner edge of the disk). Then we have for the specific angular momentum $l(r) = r^2 \Omega(r)$:

$$\dot{M} [l(r) - l(r_o)] = -2\pi r^2 W_{r\varphi}. \quad (3.1.3)$$

The torque $2\pi r^2 W_{r\varphi}$, is on the other hand, determined by Eq.(2.7.6) i.e.,

$$W_{r\varphi} = -\frac{3}{2} \Omega \int \eta dz. \quad (3.1.4)$$

In the energy equation (2.6.7) we neglect derivatives of W, S and ν_r :

$$\frac{d}{dr} \left[\dot{M} \left(\frac{1}{2} \nu_\varphi^2 - \frac{GM}{r} \right) + 2\pi r^2 W_{r\varphi} \Omega \right] = 2\pi r Q^-.$$

With Eq.(3.1.3) this becomes

$$Q^- = \frac{3}{4\pi} \dot{M} \frac{GM}{r^3} \left[1 - \left(\frac{r_0}{r} \right)^{1/2} \right] \quad (3.1.5)$$

Note that Q^- is independent of η !

This equation also follows from $Q^- = Q^+$, Eq.(23), and Eq.(36).

3.1.2 Vertical structure Equations

For the vertical structure, we have the following equations

$$\frac{dP}{dz} = -\varrho \frac{GM}{r^2} \frac{z}{r} \quad (3.1.6)$$

$$\frac{dF}{dz} = \frac{9}{4} \frac{GM}{r^3} \eta \quad (3.1.7)$$

$$P = \frac{k}{\mu m_H} \varrho T + \frac{a}{3} T^4 \quad (3.1.8)$$

$$\frac{dT}{dz} = \begin{cases} \frac{-3\kappa\varrho F}{4acT^3} & \text{for } \nabla_{rad} \leq \nabla_{ad} \\ \varrho \frac{GM}{r^2} \frac{z}{r} \frac{T}{P} \nabla_{conv} & \text{for } \nabla_{rad} > \nabla_{ad} \end{cases} \quad (3.1.9)$$

The last equation is the energy transport equation, which is well- known from the theory of stellar structure. The upper line has to be used if radiation transport is dominates and the disk is optically thick .The lower line of Eq.(3.1.9) gives roughly the energy transport if convection dominates,

The opacity is dominated by electron scattering and free- free transitions. These contributions to the total opacity κ are

$$\frac{1}{\kappa} \simeq \frac{1}{\kappa_{es}} + \frac{1}{\kappa_{ff}},$$

with

$$\kappa_{es} = 0.04m^2/Kg$$

$$\kappa_{ff} = (0.645 \times 10^{23} cm^2/g) \frac{Z^2}{A} \bar{G} \left(\frac{\rho_o}{g/cm^3} \right) T_K^{-7/2} \quad (3.1.10)$$

If the disk is optically thin , the energy in the disk is mainly lost by free- free emission .

Thus

$$Q^- = \int \varepsilon_{ff} dz \quad (\tau < 1) \quad (3.1.11)$$

$$\varepsilon_{ff} = (1.4 * 10^{-27} ergs^{-1} cm^{-3}) T^{1/2} n_e n_i Z^2 \bar{G}(T). \quad (3.1.12)$$

3.2 Standard Disks

3.2.1 Viscosity

Detailed disk models can only be constructed if we know the magnitude of the viscosity. Unfortunately, we can at best make order of magnitude estimates, since we are dealing with a highly supersonic strongly shearing fluid that is radiative, and has a large Reynolds number.

The sources of viscosity might be small- scale turbulence and transfer of angular momentum by magnetic stresses. Random magnetic fields are amplified by the differential rotation and turbulence of the disk . At the interface between adjacent cells of the resulting chaotic field , the gradient become so strong that magnetic field line reconnection occurs .

Clearly, we are not able to handle these complicated phenomena in a quantitative manner. A reasonable parametrization has, however, been given by shakura and sunyaev [1] which we discuss next.

The contribution of the turbulent part of the term $\eta \Delta \nu$ to the pressure in the Navier-stokes equation will be of the order $\eta \nu_{turb} / l_{turb}$ where ν_{turb} is the speed of the turbulent motions relative to the average motion, and l_{turb} is the characteristic size of the (largest

) turbulent cells. For fully developed turbulence, this viscous force will be comparable to the inertial force $\rho\nu_{turb}^2$. and thus

$$(3.2.1)$$

The turbulent speed ν_{turb} will be less than the sound speed c_s ; otherwise shocks would develop and quickly convert the turbulent energy in to heat , furthermore, we must require $l_{turb} \lesssim z_o$.

Consequently the turbulent part of Eq.(2.4.9) will be bounded by

$$-t_{\varphi r}^{turb} \simeq \eta_{turb}\Omega \lesssim \rho c_s z_o \Omega \simeq \rho c_s^2. \quad (3.2.2)$$

We expect the same inequality for the magnetic shear stress, because

$$-t_{\varphi r}^{mag} < P^{mag} \left(= \frac{B^2}{8\pi} \right) \lesssim P^{therm} \simeq \rho c_s^2. \quad (3.2.3)$$

Hence shakura and sunyaev propose

$$t_{r\varphi} = -\alpha P, \quad (3.2.4)$$

Where α is a free parameter, satisfying $\alpha \lesssim 1$. Models which are based on this parametrization are called " $\alpha - disks$ ". They are clearly too primitive to be more than of qualitative value.

comparison of Eq.(3.2.4) with Eq.(2.4.9) gives

$$\eta = \frac{2}{3}\alpha \left(\frac{GM}{r^3} \right)^{-1/2}. \quad (3.2.5)$$

3.2.2 vertical structure

Once a formula for the viscosity is given, we can determine with Eqs.(3.1.6 - 3.1.9) the local structure of the disk. We assume, following [35], a polytropic equation of state for fixed r ,

$$P(z) = K \rho(z)^{1+1/N}. \quad (3.2.6)$$

Equation (3.1.6) can then immediately be solved with the result

$$K(1+N)\varrho^{1/N} = \frac{1}{2} \frac{GM}{r} \left[\left(\frac{z_o}{r} \right)^2 - \left(\frac{z}{r} \right)^2 \right]. \quad (3.2.7)$$

For the values in the central plane (indexed by c) we obtained

$$P_c/\varrho_c = \frac{1}{1+N} \frac{1}{2} \frac{GM}{r} \left(\frac{z_o}{r} \right)^2. \quad (3.2.8)$$

Furthermore

$$\begin{aligned} S &= 2\varrho_c z_o I(N) \\ W &= 2P_c z_o I(N+1), \end{aligned} \quad (3.2.9)$$

where

$$I(N) = \frac{(2^N N!)^2}{(2N+1)!}. \quad (3.2.10)$$

From Eq.(3.2.4) we have generally

$$W_{r\varphi} = -\alpha W. \quad (3.2.11)$$

Next we calculate Q^- . In the optically thin case, we can use Eq.(3.1.11). If we write Eq.(3.1.12) as $\varepsilon_{ff} = \varepsilon_0 \varrho^2 T^{1/2}$, then

$$Q^- = 2\varepsilon_o \varrho_c^2 T_c^{1/2} \int_0^{z_o} \left(\frac{\varrho}{\varrho_c} \right)^2 \left(\frac{T}{T_c} \right)^2 dz.$$

With the aid of Eq.(3.2.7), the equation of state (without the radiation term in the optically thin case). And Eq.(3.2.6) we find

$$Q^- = 2\varepsilon_o J(2N) \varrho_c^2 T_c^{1/2} z_o \quad (\text{optically thin}), \quad (3.2.12)$$

Where

$$J(N) = \frac{(2N+2)!}{2^{2N+2} [(N+1)!]^2}. \quad (3.2.13)$$

For optically thick parts of the disk, we use the first equation of Eq.(3.1.9)(ignoring convection),

$$Q^- = -2 \left(\frac{4acT^3}{3\kappa\varrho} \frac{dT}{dz} \right)_{surface}. \quad (3.2.14)$$

Let us evaluate this under the assumption that either P_r , or P_g dominates in the central disk.

If the radiation pressure dominates, we obtain from the equation of state and the hydrostatic equilibrium in the z-direction immediately dT/dz and then

$$Q^- = 2 \frac{c}{\kappa} \frac{GM}{r^2} \frac{z_o}{r} \quad (\text{optically thick}, P_{rc} > P_{gc}). \quad (3.2.15)$$

For the opposite case ($P_{gc} > P_{rc}$). we use an opacity law of the form

$$\kappa = \kappa_o \varrho^n T^{-s}. \quad (3.2.16)$$

The equation of state and Eq.(3.2.6) imply

$$T = T_c \left[1 - \left(\frac{z}{z_o} \right)^2 \right].$$

Together with Eq.(3.2.7) We find

$$Q^- = \left(\frac{16acT^4}{3\kappa\varrho} \right) \frac{1}{c z_o} \left[1 - \left(\frac{z}{z_o} \right)^2 \right]_{z \rightarrow z_o}^{3+s+-N(1+n)}.$$

the limit $z \rightarrow z_o$ exists only if $N = (3 + s)/(1 + n)$ and then

$$Q^- = \left(\frac{16acT^4}{3\kappa\varrho} \right) \frac{1}{c z_o} \quad (\text{optically thick}, P_{gc} > P_{rc}). \quad (3.2.17)$$

If κ is dominated by electron scattering, then [see Eq.(3.1.10)] $N = 3$.

3.2.3 Radial structure

The vertical structure described in the previous paragraph depends on the parameters z_o and ϱ_c which are function of the radius. The radial equations in sect.3.1.1, together with the "α - laws" Eq.(3.2.11) allow us to determine these functions (for given M, \dot{M}).

From Eq.(3.1.3) and Eq.(3.2.11) we have

$$W(r) = \frac{\dot{M}}{2\pi r^2 \alpha} [l(r) - l(r_o)] \quad (3.2.18)$$

with $l(r) = \sqrt{GM}r$.

On the left hand side, we insert Eq.(3.2.9) to obtain

$$P_c(r) = \frac{1}{I(N+1)} \frac{\dot{M}}{4\pi r^2 \alpha} \left(\frac{z_o}{r}\right)^{-1} \left(\frac{GM}{r}\right)^{1/2} \left[1 - \left(\frac{r_o}{r}\right)^{1/2}\right]. \quad (3.2.19)$$

This equation contains still the parameter z_o . Using the relation Eq.(3.2.8) between ϱ_c and P_c gives

$$\varrho_c(r) = \frac{2(N+1)}{I(N+1)} \frac{\dot{M}}{4\pi r^2 \alpha} \left(\frac{GM}{r}\right)^{-1/2} \left(\frac{z_o}{r}\right)^{-3} [1 - (r_o/r)^{1/2}]. \quad (3.2.20)$$

The equation of state allows us now to express T_c as a function of r and z_o :

$$T_c = \begin{cases} \frac{1}{2(N+1)} \frac{\mu m_H}{k} \frac{GM}{r} \left(\frac{z_o}{r}\right)^2 & \text{for } P_g > P_r \\ \left[\frac{3}{a} P_c(r)\right]^{1/4} & \text{for } P_r > P_g. \end{cases} \quad (3.2.21)$$

Next we use the continuity equation Eq.(3.1.1),Eq.(3.2.9) and Eq.(3.2.20) to determine also ν_r as a function of r and z_o :

$$-\nu_r = \alpha \frac{I(N+1)}{2(N+1)I(N)} \left(\frac{GM}{r}\right)^{1/2} \left(\frac{z_o}{r}\right)^2 [1 - (r_o/r)^{1/2}]^{-1}. \quad (3.2.22)$$

This equation shows that indeed $\nu_r/\nu_\varphi = o((\frac{z_o}{r}))^2$. The previous relation imply also that $\frac{dW}{dr} / \frac{GMS}{r^2} = o((\frac{z_o}{r}))^2$. A posteriori, this justifies that we have neglected such terms at several occasions.

Finally, if we use the expression (3.1.5) for Q^- and compare it with those of the previous paragraph[Eqs.(3.2.15), (3.2.17) and (3.2.12)] the half thickness z_o of the disk is also determined . For the optically thick case we have:

$$\frac{3}{4\pi} \dot{M} \frac{GM}{r^3} [1 - (r_o/r)^{1/2}] = \begin{cases} \left(\frac{16acT^4}{3\kappa\varrho}\right)_c \frac{1}{z_o} & \text{for } P_{gc} > P_{rc} \\ 2\left(\frac{c}{\kappa} \frac{GM}{r^2}\right) \frac{z_o}{r} & \text{for } P_{rc} > P_{gc}. \end{cases} \quad (3.2.23)$$

If the disk is optically thin, the relation is

$$\frac{3}{4\pi} \dot{M} \frac{GM}{r^3} [1 - (r_o/r)^{1/2}] = 2\varepsilon_o J(2N) \varrho_c^2 T_c^{1/2} z_o. \quad (3.2.24)$$

The five algebraic equations Eqs.(3.2.19-3.2.24),together with the opacity law Eq.(3.1.10),can easily be solved in terms of r , M , and \dot{M} .

We distinguish three different regions of the disk, whose properties are given in Tables (3.1-3.3)(From[3])

we use the notation:

$$\tilde{I} = \frac{3}{2}I(N + 1), \quad (3.2.25)$$

and

$$\mathcal{J} = 1 - (r_0/r)^{1/2}.$$

Table 3.1: outer region : $P_g > P_r, \kappa \approx \kappa_{ff}$

$\frac{z_0}{r} = 7.7 \times 10^{-3} \frac{(N+1)^{19/40}}{\tilde{I}^{1/10}} \alpha^{-1/10} (2\mu)^{-3/8} \left(\frac{3r_g}{r_0}\right)^{-1/8} \left(\frac{M}{M_\odot}\right)^{-1/4} \dot{M}_{17}^{3/20} \left(\frac{r}{r_0}\right)^{1/8} \mathcal{J}^{3/20}$
$T_c = (2.7 \times 10^7 \text{ K}) \frac{(N+1)^{-1/20}}{\tilde{I}^{1/5}} \alpha^{-1/5} (2\mu)^{1/4} \left(\frac{3r_g}{r_0}\right)^{3/4} \left(\frac{M}{M_\odot}\right)^{-1/2} \dot{M}_{17}^{3/10} \left(\frac{r}{r_0}\right)^{-3/4} \mathcal{J}^{3/10}$
$\rho_c = (5.3 \text{ g cm}^{-3}) \frac{(N+1)^{-17/40}}{\tilde{I}^{7/10}} \alpha^{-7/10} (2\mu)^{9/8} \left(\frac{3r_g}{r_0}\right)^{15/8} \left(\frac{M}{M_\odot}\right)^{-5/4} \dot{M}_{17}^{11/20} \left(\frac{r}{r_0}\right)^{-15/8} \mathcal{J}^{11/20}$
<p>Optical depth:</p>
$\tau_{\text{ff}} = 122 \frac{(N+1)^{-1/5}}{\tilde{I}^{4/5}} \alpha^{-4/5} (2\mu) \dot{M}_{17}^{1/5} \mathcal{J}^{1/5} > 1$
$\tau_{\text{es}} = 1.5 \times 10^4 \frac{(N+1)^{1/20}}{\tilde{I}^{4/5}} \alpha^{-4/5} (2\mu)^{3/4} \left(\frac{3r_g}{r_0}\right)^{3/4} \left(\frac{M}{M_\odot}\right)^{-1/2} \dot{M}_{17}^{7/10} \left(\frac{r}{r_0}\right)^{-3/4} \mathcal{J}^{7/10}$
<p>Inner boundary ($\tau_{\text{ff}} = \tau_{\text{es}}$) at:</p>
$\frac{r}{r_0} = 6.0 \times 10^2 (N+1)^{1/3} (2\mu)^{-1/3} \left(\frac{3r_g}{r_0}\right) \left(\frac{M}{M_\odot}\right)^{-2/3} \dot{M}_{17}^{2/3}$

Table 3.2: Middle region : $P_g > P_r, \kappa \approx \kappa_{es}$

$$\frac{z_0}{r} = 1.2 \times 10^{-2} \frac{(N+1)^{1/2}}{\tilde{I}^{1/10}} \alpha^{-1/10} (2\mu)^{-2/5} \left(\frac{3r_g}{r_0}\right)^{-1/20} \left(\frac{M}{M_\odot}\right)^{-3/10} \dot{M}_{17}^{1/5} \left(\frac{r}{r_0}\right)^{1/20} \mathcal{J}^{1/5}$$

$$T_c = (6.5 \times 10^7 \text{ K}) \tilde{I}^{-1/5} \alpha^{-1/5} (2\mu)^{1/5} \left(\frac{3r_g}{r_0}\right)^{9/10} \left(\frac{M}{M_\odot}\right)^{-3/5} \dot{M}_{17}^{2/5} \left(\frac{r}{r_0}\right)^{-9/10} \mathcal{J}^{2/5}$$

$$\rho_c = (1.4 \text{ g cm}^{-3}) \frac{(N+1)^{-1/2}}{\tilde{I}^{7/10}} \alpha^{-7/10} (2\mu)^{6/5} \left(\frac{3r_g}{r_0}\right)^{33/20} \left(\frac{M}{M_\odot}\right)^{-11/10} \dot{M}_{17}^{2/5} \left(\frac{r}{r_0}\right)^{-33/20} \mathcal{J}^{2/5}$$

$$\left(\frac{P_g}{P_r}\right)_c = 0.3 \frac{(N+1)^{-1/2}}{\tilde{I}^{1/10}} \alpha^{-1/10} (2\mu)^{-2/5} \left(\frac{3r_g}{r_0}\right)^{-21/20} \left(\frac{M}{M_\odot}\right)^{7/10} \dot{M}_{17}^{-4/5} \left(\frac{r}{r_0}\right)^{21/20} \mathcal{J}^{-4/5}$$

Inner boundary ($P_g = P_r$) at:

$$\frac{r}{r_0} \mathcal{J}(r)^{-16/21} = 3.2 \frac{(N+1)^{10/21}}{\tilde{I}^{-2/21}} \alpha^{2/21} (2\mu)^{8/21} \left(\frac{3r_g}{r_0}\right) \left(\frac{M}{M_\odot}\right)^{-2/3} \dot{M}_{17}^{6/21}$$

Table 3.3: Inerr region : $P_r > P_g, \kappa \approx \kappa_{es}$

$$\frac{z_0}{r_0} = 0.2 \left(\frac{3r_g}{r_0} \right) \left(\frac{M}{M_\odot} \right)^{-1} \dot{M}_{17} \mathcal{J}$$

$$T_c = (2.5 \times 10^7 \text{ K}) \tilde{I}^{-14} \alpha^{-1/4} \left(\frac{3r_g}{r_0} \right)^{3/8} \left(\frac{M}{M_\odot} \right)^{-1/4} \left(\frac{r}{r_0} \right)^{-3/8}$$

$$\rho_c = (3.5 \times 10^{-4} \text{ g cm}^{-3}) \frac{(N+1)}{\tilde{I}} \alpha^{-1} \left(\frac{3r_g}{r_0} \right)^{-3/2} \left(\frac{M}{M_\odot} \right) \dot{M}_{17}^{-2} \left(\frac{r}{r_0} \right)^{3/2} \mathcal{J}^{-2}$$

Optical depth τ_c :

$$\tau_c = 1.6 \frac{(N+1)}{\tilde{I}} \alpha^{-1} \left(\frac{3r_g}{r_0} \right)^{-1/2} \left(\frac{M}{M_{cr}} \right)^{-1} \left(\frac{r}{r_0} \right)^{3/2} \mathcal{J}^{-1}$$

Ratio of radial to azimuthal velocity:

$$-v_r/v_\phi = 3\alpha \frac{\tilde{I}}{(N+1)I(N)} \left(\frac{M}{M_{cr}} \right)^2 \left(\frac{r_0}{r} \right)^2 \mathcal{J}$$

(i). For $r \rightarrow r_o$ the solution for the inner region becomes unphysical: $\nu_r \rightarrow 0$, $\rho_c \rightarrow \infty$.

(ii). T_c is independent of \dot{M} in the inner region.

(iii). From our solution, we can determine the viscosity as a function of r, α, M and \dot{M} . for instance , in the inner zone , we find From $Q^+ = Q^-$ and expressions Eq.(3.1.1) for Q^+ and Eq.(3.2.15) for Q^- :

$$\frac{9}{4} \frac{GM}{r^3} \int \eta dz = 2 \frac{c}{\kappa} \frac{GM}{r^2} \frac{z_o}{r}$$

and thus

$$\eta = \frac{4}{9} \frac{cm_p}{\sigma_T} = 3.5 \times 10^{10} \text{ erg s cm}^{-3}. \quad (3.2.26)$$

Surprisingly, this value is independent of all parameters of the accretion. It is Instructive to compare it with the radiative viscosity

$$\eta_{rad} = \frac{4}{15} \frac{aT^4}{\sigma_T n_e c}, \quad (3.2.27)$$

For a derivation see, e.g [36], this shows that the maximum value of radiative viscosity Eq.(3.2.27) in the inner region is always much smaller than Eq.(3.2.26).

Chapter 4

Stability Analysis Of Thin Accretion Disks

We investigate now, following the work of shakura and sunyaev [3] The stability of the stead disks described in sect. 3.2. only stable models have a chance to be physically relevant. It will turn out that possible instabilities depends strongly on the assumed viscosity.

We consider only axially symmetric perturbations of wavelength Λ , satisfying $z_o \ll \Lambda \ll r$,and which change little on the dynamic time scale Ω^{-1} . (Remember that Ω^{-1} is also roughly the time it takes for a sound wave to cross the disk in the transverse direction.)

The basic time-dependent equations have been derived in sect 2. For a linear stability analysis, We have to linearize these equation around the equilibrium solutions.

For the type of perturbations, which we want to consider, we can still use in the vertical direction the hydrostatic equation (neglecting terms of order $(z_o/r)^2$. Further more, ν_φ is still keplerian, up to terms of order $(z_o/r)^2, z_o^2/r\Lambda$.

4.1 Dynamic Equation

In the Keplerian approximation for ν_φ we get from Eq.(2.4.8), since ν_φ is time independent,

$$rS\nu_r = \frac{\partial_r(r^2W_{r\varphi})}{\partial_r(r\nu_\varphi)}. \quad (4.1.1)$$

According to Eq.(2.7.6) we have, if $\nu = \eta/\rho$ denotes the kinematic viscosity,

$$\begin{aligned} W_{r\varphi} &= r \frac{d\Omega}{dr} \int \nu \rho dz. \\ &= r \frac{d\Omega}{dr} \nu S \end{aligned} \quad (4.1.2)$$

Hence, we obtain from Eq.(4.1.1)

$$r\nu_r S = -\frac{3}{r\Omega} \partial_r [\nu r^2 \Omega S]. \quad (4.1.3)$$

Applying on this equation the operator $r^{-1}\partial_r$ and using the continuity equation (2.3.4) gives the following interesting diffusion type equation for S :

$$\partial_t S = \frac{3}{r} \partial_r \left\{ \frac{1}{r\Omega} \partial_r [\nu S r^2 \Omega] \right\}. \quad (4.1.4)$$

4.2 Thermal Equation

Instead of Eq.(2.6.2) we use another form of energy from the energy equation, which we derive now.

The starting point is Eq.(A.21), Which we write as as follows

$$D_t(\varepsilon \rho) - (\varepsilon \rho + P) \frac{D_t \rho}{\rho} = \Upsilon - \text{div} q$$

or, using the continuity equation

$$\partial_t(\rho \varepsilon) + \text{div}[(\varepsilon \rho + P)\nu] - \nabla_\nu P = \Upsilon - \text{div} q.$$

Thus

$$\partial_t(\rho \varepsilon) + \frac{1}{r} \partial_r [r\nu_r(\varepsilon \rho + P)] + \partial_z [\nu_z(\varepsilon \rho + P)] - \nu_r \partial_r P - \nu_z \partial_z P = \Upsilon - \text{div} q.$$

Integrating over z gives

$$\partial_t \int \rho \varepsilon dz + \frac{1}{r} \partial_r \left(\int r\nu_r(\varepsilon \rho + P) dz \right) - \int \nu_r \partial_r P dz - \int \nu_z \partial_z P dz = Q^+ - Q^-. \quad (4.2.1)$$

This equation is so far exact. Now by Eq.(2.2.2)

$$\varrho\varepsilon = AP, \quad A = \frac{\beta}{\gamma - 1} + 3(1 - \beta).$$

In the thin disk approximation and using the hydrostatic equation for $\partial_z P$, we obtain

$$\partial_t(AW) + \frac{1}{r}\partial_r[r\nu_r(A+1)W] - \nu_r\partial_r W + \Omega^2 \int \varrho\nu_z z dz = Q^+ - Q^-. \quad (4.2.2)$$

From Eq.(2.7.9) we have also

$$Q^+ = \frac{9}{4}\nu S\Omega^2. \quad (4.2.3)$$

For the $\alpha - model$, Eq.(3.2.5) gives

$$\nu = \frac{2\alpha}{3} \frac{W}{S} \frac{1}{\Omega}. \quad (4.2.4)$$

The expression (3.2.14) for Q^- is also valid in the perturbed situation. we write this equation as [see also Eq.(3.2.17)] :

$$Q^- = e_s \frac{8}{3} \left(\frac{acT^4}{\kappa} \right) \frac{1}{cS}, \quad (4.2.5)$$

Where e_s is a structure factor, which depends on the detailed vertical structure of the disk.

From now on, we choose for simplicity (as in [3]) a constant density in the z-direction and assume that the perturbations in the z- direction preserve this property.

Then the hydrostatic equation in the z-direction gives

$$P(z) = P_c \left[1 - \left(\frac{z}{z_o} \right)^2 \right], \quad P_c = \frac{1}{4} S \Omega^2 z_o \quad (4.2.6)$$

and thus the average pressure is

$$P = \frac{1}{6} S \Omega^2 z_o. \quad (4.2.7)$$

We also have

$$W = \frac{4}{3} P_c z_o = \frac{1}{3} S \Omega^2 z_o^2 \quad (4.2.8)$$

and thus from Eq.(4.2.4) for the $\alpha - models$

$$\nu = \frac{2}{9}\alpha\Omega^2 z_o^2, \quad (4.2.9)$$

Furthermore, since $\nu_z = \frac{z}{z_o}\partial_t z_o$,

$$\int \varrho \nu_z z dz = \frac{1}{3} S z_o \partial_t z_o.$$

Inserting these expressions into Eq.(4.2.2) gives

$$\begin{aligned} & \frac{1}{3}\partial_t[AS\Omega^2 z_o^2] + \frac{1}{3}\frac{1}{r}\partial_r[r\nu_r(A+1)S\Omega^2 z_o^2] \\ & - \frac{1}{3}\nu_r\partial_r(S\Omega^2 z_o^2) + \frac{1}{3}S\Omega^2 z_o\partial_t z_o = Q^+ - Q^-. \end{aligned} \quad (4.2.10)$$

In the second term on the left we use Eq.(4.1.3) to get the basic equation :

$$\begin{aligned} & \frac{1}{3}\partial_t[AS\Omega^2 z_o^2] - \frac{1}{r}\partial_r\left\{(A+1)\frac{\Omega z_o^2}{r}\partial_r[\nu\Omega r^2 S]\right\} \\ & - \frac{1}{3}\nu_r\partial_r(S\Omega^2 z_o^2) + \frac{1}{3}S\Omega^2 z_o\partial_t z_o = Q^+ - Q^-. \end{aligned} \quad (4.2.11)$$

4.3 Linearization

Equations Eq.(4.1.4) and Eq.(4.2.11) have to be linearized now around the equilibrium.

Let us introduce the following notations for the changes of S and z_o from their equilibrium values

$$\frac{\delta S}{S} = u, \quad \frac{\delta z_o}{z_o} = h, \quad |u|, |h| \ll 1. \quad (4.3.1)$$

We set

$$\frac{\delta \nu}{\nu} = nu + mh + \dots \quad (4.3.2)$$

If we use the $\alpha - law$ Eq.(4.2.9), then

$$n = 0, \quad m = 2. \quad (4.3.3)$$

Inserting Eq.(4.3.1) and Eq.(4.3.2) gives for the linearization of Eq.(4.1.4)

$$S\partial_t u = 3\nu S\partial_r^2[(n+1)u + mh]. \quad (4.3.4)$$

The linearization of Eq.(4.2.11) is a bit more complicated.

Let

$$\frac{\delta Q^-}{Q^-} = lu + kh + \dots, \quad (4.3.5)$$

where the expansion coefficients depend on the opacity κ . one must also include variations of A . For definiteness we choose $\gamma = \frac{5}{3}$. Then

$$A = \frac{3}{2}(1 + \beta_o), \quad \beta_o \equiv 1 - \beta. \quad (4.3.6)$$

(Note that β in [3] is our β_o .) First-order changes of β_o are obtained from equation of state,

$$P = \beta_o P + \frac{k}{\mu m_H} \frac{S}{2z_o} \left(\frac{3\beta_o P}{a} \right)^{1/4}$$

and from the expression (4.2.7) for P . Computing the variations of these two equations gives

$$\frac{\delta \beta_o}{\beta_o} = \frac{1 - \beta_o}{1 + 3\beta_o} (7h - u). \quad (4.3.7)$$

Now the linearization of Eq.(4.2.11) is straight forward. Using the equilibrium conditions (in particular $Q^+ = Q^-$), one finds for the α - model, if only the dominant terms of order $(z_o/\Lambda)^2$ are kept:

$$\begin{aligned} & 3(1 + 3\beta_o + 4\beta_o^2)\partial_t u + (8 + 51\beta_o \\ & - 3\beta_o^2)\partial_t h - 3(1 + 3\beta_o)\alpha\Omega[(n + 1 - l)u + (m - k)h] \\ & = \frac{2}{3}\alpha\Omega z_o^2(5 + 18\beta_o + 9\beta_o^2)\partial_r^2[(n + 1)u + mh]. \end{aligned} \quad (4.3.8)$$

If $\kappa \approx \kappa_{es}$ we have from Eq.(4.2.5) and Eq.(4.2.6)

$$Q^- = e_s \frac{8m_p c \beta_o P_c}{\sigma_T S} = 2e_s \frac{m_p c}{\sigma_T} \beta_o z_o \Omega^2. \quad (4.3.9)$$

Thus

$$\frac{\delta Q^-}{Q^-} = \frac{\delta \beta_o}{\beta_o} + h.$$

Using Eq.(4.3.7) this gives

$$k = \frac{8 - 4\beta_o}{1 + 3\beta_o}, \quad l = \frac{\beta_o - 1}{1 + 3\beta_o}, \quad (4.3.10)$$

All perturbations are fully described by Eq.(4.3.4) and Eq.(4.3.8), since all quantities of interest, in particular \dot{M} , can be expressed in terms of u and h .

We consider harmonic perturbations

$$u(r, t) = u(r)e^{wt}, \quad h(r, t) = h(r)e^{wt}$$

and write a single equation for the combination

$$\Psi = (n + 1)u + mh. \quad (4.3.11)$$

This amplitude describes the viscous perturbations, as can be seen from Eq.(4.2.3), Eq.(4.3.1) and Eq.(4.3.2).

From Eq.(4.3.4) we get for the $\alpha - law$

$$u = \frac{2}{3}\alpha \frac{\Omega}{\omega} z_o^2 \partial_r^2 \Psi. \quad (4.3.12)$$

Using Eq.(4.3.11), Eq.(4.3.12) in Eq.(4.3.8) gives

$$\omega \frac{A\omega - 3(1 + 3\beta_o)\alpha\Omega(m - k)}{B\omega - 3(1 + 3\beta_o)\alpha\Omega[ml - k(n + 1)]} \Psi = \frac{2}{3}\alpha\Omega z_o^2 \partial_r^2 \Psi, \quad (4.3.13)$$

where

$$\begin{aligned} A(\beta_o) &= 8 + 51\beta_o - 3\beta_o^2 \\ B(\beta_o) &= (n + 1)A(\beta_o) + m(2 + 9\beta_o - 3\beta_o^2). \end{aligned} \quad (4.3.14)$$

For solutions proportional to $\sin(r/\Lambda)$ we obtain the dispersion relation

$$\begin{aligned} A\left(\frac{\omega}{3\alpha\Omega}\right)^2 + \left[2B\left(\frac{z_o}{3\Lambda}\right)^2 - (1 + 3\beta_o)(m - k)\right] \frac{\omega}{3\alpha\Omega} \\ - 2\left(\frac{z_o}{3\Lambda}\right)^2 (1 + 3\beta_o)[ml - (n + 1)k] = 0. \end{aligned} \quad (4.3.15)$$

This agrees with Eq.(4.14) of [3] for the special values Eq.(4.3.3) and Eq.(4.3.10).For these we obtain

$$\frac{\omega}{\alpha\Omega} = \frac{3}{A} \left\{ - \left[B \left(\frac{z_o}{3\Lambda} \right)^2 + (3 - 5\beta_o) \right] \pm \left[\left(B \left(\frac{z_o}{3\Lambda} \right)^2 + (3 - 5\beta_o) \right)^2 - 4A(5 - 3\beta_o) \left(\frac{z_o}{3\Lambda} \right)^2 \right]^{1/2} \right\} \quad (4.3.16)$$

with

$$A(\beta_o) = 8 + 51\beta_o - 3\beta_o^2 > 0, \quad B(\beta_o) = 3(4 + 23\beta_o - 3\beta_o^2) > 0. \quad (4.3.17)$$

Obviously, $Re\{\omega\} < 0$, if $3 - 5\beta_o > 0$. We thus have stability for $\beta_o < \frac{3}{5}$, Which is the case if the plasma pressure dominates.

And $Re\{\omega\} > 0$, if $3 - 5\beta_o < 0$, which is the case if the radiation pressure dominates.

When the radiation pressure dominates ($\beta_o > \frac{3}{5}$) there is an unstable mode for Λ/z_o larger than some value which depends on β_o .

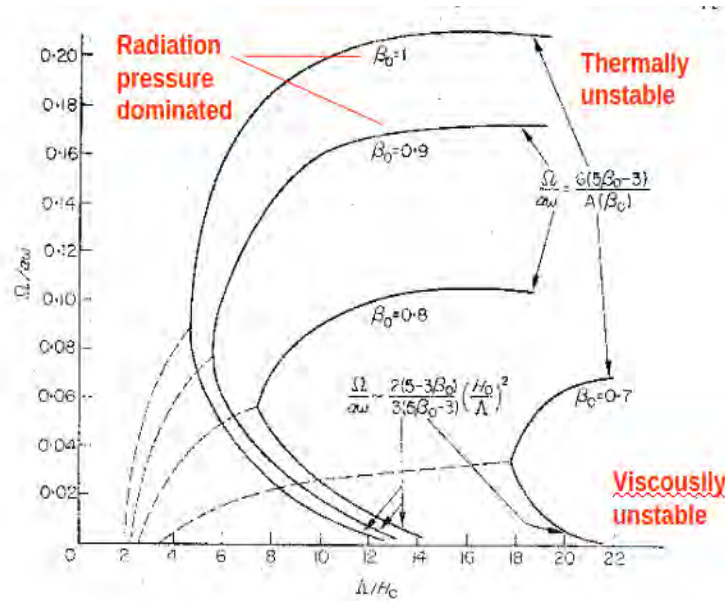


Figure 4.1: Instability growth rate when radiation pressure dominates ($\beta_o > \frac{3}{5}$) as a function of wavelength Λ . Broken lines denote traveling waves, continuous lines denotes standing waves. Upper branches correspond to thermal instabilities and lower branches to dynamic instabilities.(from[3]).

For ($\beta_o = 1$) this minimum value is equal to 2. This unstable mode bifurcates at higher value of Λ/z_o , as shown in fig.4.1.

The two branches correspond to physically quite distinct instabilities. For the lower branch the perturbed viscosity becomes for long wavelengths very small ($Q^+ \approx Q^-$). On the other branch, the perturbation of the surface density becomes small compared to the viscous forces, disk thickness and other quantities. The growth of these perturbations is due to a thermal instability ($Q^+ \neq Q^-$). For a detailed discussion, we refer to [3].

If one uses a modified α -law for which the viscosity is taken proportional to the gas pressure, instead of the total pressure, then one finds a dispersion relation which shows no instability. This illustrates that it is dangerous to draw definite conclusions from the previous analysis.

4.4 Estimating The Radius of Instability Of The Inner Region Of The Disk

To estimate the radius of instability of the inner region of the disk in which radiation pressure and electron scattering opacity dominates, first let us express its instability condition in terms of β , where β is the ratio of gas pressure to the total pressure of the disk.

i.e

$$\beta = \frac{P_g}{P_g + P_r} < \frac{2}{5} \quad \text{since} \quad \beta_o = 1 - \beta \quad (4.4.1)$$

where P_g and P_r are gas pressure and radiation pressure respectively, which are given by

$$\begin{aligned} P_g &= \frac{\rho_c k_B T_c}{\bar{\mu} m_H} \\ P_r &= \frac{1}{3} a T_c^4 \end{aligned} \quad (4.4.2)$$

where $\bar{\mu}$ ($= 0.62$) the mean molecular weight for a fully ionized hydrogen gas, m_H is mass of hydrogen atom which is equivalent to the mass of a proton (m_p).

And a is radiation constant related to the total energy radiated by a blackbody (i.e.,

the Stefan-Boltzmann law), and defined as

$$\begin{aligned} a &\equiv \frac{4\sigma}{c} \\ &= \frac{8\pi^5 k_B^4}{15c^3 h^3}, \end{aligned} \quad (4.4.3)$$

where σ is the Stefan-Boltzmann constant, c is the speed of light, k_B is Boltzmann's constant, and h is Planck's constant. Numerically,

$$k_B = 1.3807 \times 10^{-23} J.K^{-1}$$

$$c = 3 \times 10^8 m/s$$

$$\sigma = 5.6704 \times 10^{-8} W.m^{-2}K^{-4}$$

$$h = 6.6261 \times 10^{-34} J.s$$

$$a = 7.5657 \times 10^{-16} Jm^{-3}K^{-4}$$

Now using Eq.(4.4.1) we can write the instability condition in the inner region in terms of radiation pressure and gas pressure.i.e

$$2P_r - 3P_g > 0 \quad (4.4.4)$$

putting in the expansions for p_r and p_g , this gives

$$\frac{2}{3}aT_c^4 - \frac{3\rho_c k_B T_c}{\mu m_p} > 0 \quad (4.4.5)$$

But to express equation (4.4.5) as a function of radius "r" , it is necessary to write T_c and ρ_c as a function "r".

The central temperature of the inner region of the disk is given in table(3).

i.e

$$T_c = (2.5 \times 10^7 K) \tilde{I}^{-14} \alpha^{-1/4} \left(\frac{3r_g}{r_o} \right)^{3/8} \left(\frac{M}{M_\odot} \right)^{-1/4} \left(\frac{r}{r_o} \right)^{-3/8} \quad (4.4.6)$$

where

$$\begin{aligned}\tilde{I} &= \frac{3}{2}I(N+1) \\ I(N) &= \frac{(2^N N!)^2}{(2N+1)!} \\ \tilde{I} &\approx 0.61\end{aligned}\tag{4.4.7}$$

since $N = 3$ for a region dominated by electron scattering opacity ($\kappa \approx \kappa_{es}$).

The gravitational radius is defined by,

$$r_g = \frac{2GM}{c^2}\tag{4.4.8}$$

Using the fiducial model, we take a neutron star of $M = 1.4M_\odot$, and the dimensionless parameter $\alpha = 0.01$ to rewrite T_c as

$$T_c = 3.47M_\odot^{3/8}r^{-3/8}\tag{4.4.9}$$

where M_\odot is Solar mass ($M_\odot = 1.989 \times 10^{30}K.g$).

The central density (ρ_c) of the inner region as a function of "r", can be driven using the radiative energy transport equation.i.e

$$\frac{dT(r)}{dr} = \frac{-3}{16\pi ac} \frac{\kappa_{es}\rho_c(r)L}{r^2T_c^3(r)}\tag{4.4.10}$$

where $\kappa_{es} = 0.04m^2K.g^{-1}$ and L is the luminosity due to radiation, which is given by,

$$L = \frac{2\pi^5k_B^4T_c^4}{15h^3c^2}\tag{4.4.11}$$

Now using Eq.(4.4.1),Eq.(4.4.10) and Eq.(4.4.11),we obtain

$$\rho_c = \frac{8\pi}{\kappa_{es}}r\tag{4.4.12}$$

By substituting Eq.(4.4.9) and Eq.(4.4.12) into Eq.(4.4.3),we then find the equation for the critical radius at which instability occurs as:

$$\left(\frac{1.16 \times 10^2 M_\odot^{9/8} a \kappa_{es} \bar{\mu} m_p}{\pi k_B} - r^{17/8}\right)r^{-3/2} > 0\tag{4.4.13}$$

This implies,

$$0 < r < \left(\frac{1.16 \times 10^2 M_{\odot}^{9/8} a \kappa_{es} \bar{\mu} m_p}{\pi k_B} \right)^{8/17}. \quad (4.4.14)$$

But

$$\left(\frac{1.16 \times 10^2 M_{\odot}^{9/8} a \kappa_{es} \bar{\mu} m_p}{\pi k_B} \right)^{8/17} \approx 10 R_A \quad (4.4.15)$$

where R_A is an Alfven radius , the radius at which the pressure due to the pulsar's magnetic field equals the ram pressure of in falling material. Numerically, $R_A \approx 10^6 m$

There fore, the radius of instability of the inner region of the disk is less than $10 R_A$ and greater than the inner radius (r_o) of the disk. Because the disk extends from an inner radius of $\sim 10^6 m$ to an outer radius of $\sim 10^8 m$ [3].

Chapter 5

conclusion

When the ratio of radiation pressure to the total pressure is greater than the ratio three to five ($\beta_o > 3/5$), then mechanical instability is set up. Because the real part of the frequency of Eq.(4.3.16) is less than zero. This causes the loosely attached particles are removed away from the surface of the disk.

This occurred in the inner region of the disk in between the radius R_A and $10R_A$, in which radiation pressure and electron scattering opacity is dominated.

Appendix

Non Relativistic Hydrodynamics of Viscous Fluids

We develop here briefly the principal equations of fluid dynamics from a phenomenological (continuum) viewpoint. For a detailed treatment we refer to [3].

Let $\nu(x, t)$ be the velocity field and $\varrho(x, t)$ the matter density. The material (or substantial) derivative of a function f is defined by

$$D_t f = \partial_t f + L_\nu f \tag{A.1}$$

We decompose the velocity-gradient tensor (in Euclidean coordinates) as

$$\nu_{i,k} = \theta_{ik} + \omega_{ik}, \tag{A.2}$$

where

$$\theta_{ik} = \frac{1}{2}(\nu_{i,k} + \nu_{k,i}) \tag{A.3}$$

is the rate -of- deformation tensor and

$$\omega_{ik} = \frac{1}{2}(\nu_{i,k} - \nu_{k,i}) \tag{A.4}$$

is the spine-tensor.

Denote by $\phi_t(x) = \phi(x, t)$ the trajectory of a fluid particle that is at position x at time $t = 0$.

The conservation of mass says that for nice domain $D \subset \mathbb{R}^3$

$$\int_{\phi_t(D)} \varrho \eta = \int_D \varrho \eta, \tag{A.5}$$

where η is the volume of \mathbb{R}^3 (as a three-dimensional Riemannian manifold).

using the change-of-variable formula and the definition of the Lie Derivative,(A.5)for any D is equivalent to

$$\frac{\partial \varrho}{\partial t} \eta + L_\nu(\varrho \eta) = 0.$$

But

$$L_\nu(\varrho \eta) = (L_\nu \varrho) \eta + \varrho L_\nu \eta = (L_\nu \varrho + \varrho \operatorname{div} \nu) \eta$$

and thus we have the continuity equation

$$D_t \varrho + \varrho \operatorname{div} \nu = 0 \tag{A.6}$$

or equivalently,

$$\partial_t \varrho + \operatorname{div}(\varrho \nu) = 0 \tag{A.6'}$$

As a corollary, we obtain the *transport theorem* :

$$\frac{d}{dt} \int_{\phi_t(D)} \varrho f dV = \int_{\phi_t(D)} \varrho D_t f dV. \tag{A.7}$$

Indeed, as before we first get

$$\frac{d}{dt} \int_{\phi_t(D)} \varrho f dV = \int_{\phi_t(D)} [\partial_t(\varrho f) + L_\nu(\varrho f) + \varrho f \operatorname{div} \nu] dV.$$

But the bracket is, with (A.6),equals to $\varrho D_t f$.

Next we formulate the balance of momentum in integral form. we consider again a comoving fluid element in $\phi_t(D)$. The forces which act on it are of two types. The first kind are external, or body forces, such as gravity or magnetic field which exert a force per unit volume on the continuum. The second kind of force consists of a surface force, which represents the action of the rest of the continuum through the surface of a fluid element. These stress

forces are represented by the last term of the following momentum balance equation (G is the body force density):

$$\frac{d}{dt} \int_{\phi_t(D)} \rho \nu dV = \int_{\phi_t(D)} \rho G dV + \int_{\partial\phi_t(D)} T(n) dS, \quad (\text{A.8})$$

where n is the out ward unit normal. one can show that the Cauchy traction vector $T(n)$ depends linearly on n (Cauchy Lemma):

$$T_i(n) = T_{ik} n_k. \quad (\text{A.9})$$

with the transport theorem (A.7) and Gauss' theorem we find from (A.8)

$$\rho D_t \nu_i = \rho G_i + T_{ik,k}. \quad (\text{A.10})$$

This holds in Cartesian coordinate, for which $L_\nu \nu_i = (\nabla_\nu \nu)_i$. Thus the invariant form of (A.10) reads

$$\partial_t \nu + \nabla_\nu \nu = G + \frac{1}{\rho} \text{div} T. \quad (\text{A.11})$$

one can show easily that these equations of motion are compatible with angular momentum conservation for the fluid element in $\phi_t(D)$ If and only if T_{ik} is symmetric. (we exclude strongly polar media.)

We decompose T_{ik} into an isotropic pressure term and a viscous part t_{ik} which is due to velocity gradients

$$T_{ik} = -P \delta_{ik} + t_{ik}. \quad (\text{A.12})$$

since ω_{ik} represents a rigid rotation, the viscous-tenser t_{ik} will be a linear function of ϕ_{ik} . If We consider only isotropic media, we have the following decomposition into irreducible parts :

$$t_{ik} = 2\eta \sigma_{ik} + \zeta \theta \delta_{ik}, \quad (\text{A.13})$$

where

$$\sigma_{ik} = \theta_{ik} - \frac{2}{3}\delta_{ik}\theta \quad (\text{A.14})$$

is trace-free and

$$\theta = \theta_{kk} = \text{div}\nu. \quad (\text{A.15})$$

In the stress law (A.13) η is the shear viscosity and ζ the bulk viscosity.

Finally we consider various equivalent formulations of energy conservation.

The rate of energy increase for a material volume $\phi_t(D)$ is equal to the rate at which is energy is transferred to the volume via work and heat :

$$\begin{aligned} \frac{d}{dt} \int_{\phi_t(D)} \rho(\epsilon + \frac{1}{2}\nu^2)dV &= \int_{\phi_t(D)} \rho G \cdot \nu dV + \int_{\phi_t(D)} \rho T(n) \cdot \nu dS \\ &\quad - \int_{\phi_t(D)} \rho q \cdot n dS. \end{aligned} \quad (\text{A.16})$$

Here, ϵ is the specific internal energy and q in the last term is the heat flux.

Using again the transport theorem, the differential formulation of (A.16) reads,with Gauss' theorem,

$$\rho D_t(\frac{1}{2}\nu^2 + \epsilon) = \rho G \cdot \nu + \text{div}(T \cdot \nu) - \text{div}q. \quad (\text{A.17})$$

For another form of this energy equation we write the second term on the right-hand side with the help of the equation of motion (A.10) as follows

$$\begin{aligned} \text{div}(T \cdot \nu) &= \partial_k(\nu_i T_{ik}) = \nu_{i,k} T_{ik} + \nu_i T_{ik,k} \\ &= \nu_{i,k} T_{ik} + \rho \nu_i D_t \nu_i - \rho G_i \nu_i \\ &= \frac{1}{2} \rho D_t \nu^2 + \nu_{i,k} T_{ik} - \rho G_i \nu_i. \end{aligned}$$

Using this in (A.17) gives

$$\rho D_t \epsilon = T_{ik} \theta_{ik} - \text{div} q \quad (\text{A.18})$$

or, with the decomposition (A.12)

$$\rho D_t \epsilon = -P \text{div} \nu - \text{div} q + \Upsilon, \quad (\text{A.19})$$

where the dissipation function Υ is given by

$$\Upsilon = \text{Tr}(t\theta) = 2\eta \text{Tr}\sigma^2 + \zeta\theta^2 \geq 0. \quad (\text{A.20})$$

This represents the part of the viscous work going into the deformation of a fluid particle.

With Eq.(A.6) we can also write Eq.(A.19) in the form

$$\rho \left[D_t \epsilon + P D_t \frac{1}{\rho} \right] = -\text{div} q + \Upsilon. \quad (\text{A.21})$$

We now introduce the Gibbs equation

$$T ds = d\epsilon + P d(1/\rho), \quad (\text{A.22})$$

Which allows us to write (A.21) as

$$T \rho D_t s = -\text{div} q + \Upsilon. \quad (\text{A.23})$$

We next derive still another alternative form of the energy equation. we start from (A.17) and write this time

$$\begin{aligned} \text{div}(T \cdot \nu) &= -(P \nu_k)_{,k} + (t_{ik} \nu_k)_{,i} \\ &= -\nu_i P_{,i} + \frac{P}{\rho} D_t \left(\frac{1}{\rho} \right) + (t_{ik} \nu_k)_{,k}. \end{aligned}$$

After a few manipulations we obtain from (A.17)

$$\rho D_t S \left(\epsilon + \frac{P}{\rho} + \frac{1}{2} \nu^2 \right) = \partial_t P + (t_{ik} \nu_{ik})_{,i} + \rho G \cdot \nu - \text{div} q. \quad (\text{A.24})$$

If furthermore, $G = -grad\phi$, and ϕ is stationary, then

$$\rho D_t S \left(\frac{1}{2} \nu^2 + h + \phi \right) = \partial_t P + (t_{ik} \nu_{ik})_{,i} - div q. \quad (A.25)$$

Here, $h = \epsilon + P/\rho$ is the specific enthalpy. Equation (A.25) contains all the various equations which are called Bernoulli's equation. For example, if the flow is steady and inviscid ($t=0, q=0$) then (A.25) implies that $\frac{1}{2} \nu^2 + h + \phi$ is constant on any given streamline.

Finally we write down the constitutive relation between heat flux and temperature gradient,

$$q = \chi grad T, \quad (A.26)$$

which is known as the Fourier heat conduction law.

References

- [1] Shakura, N.I. and Sunyaev, R.A.: 1973, *Astron. Astrophys.* 24, 317,337.
- [2] Pringle, J.E., Rees, M.J. and Pacholczyk, A.G.: 1973, *Astron. Astrophys.* 29, 179.
- [3] Shakura, N.I. and Sunyaev, R.A.: 1976, *Mon. Not. R. Astron. Soc.* 175, 613.
- [4] Lightman, A. and Eardley, D.: 1974, *Astrophys. J.* 187, L1.
- [5] Lin, D.N.C. and Papaloizou, J.C.B.: 1996, *Ann. Rev.* 33, 504.
- [6] Blumenthal, G.R., Yang, L.T. and Lin, D.N.C.: 1984, *Astrophys. J.* 287, 774.
- [7] Okuda, T., Ono, K., Tabata, M. and Mineshigs, S.: 1992, *Mon. Not. R. Astron. Soc.* 254, 427.
- [8] Chen, X. and Tamm, R.E.: 1995, *Astrophys. J.* 441, 354.
- [9] Piran, T.: 1978, *Astrophys. J.* 221, 652.
- [10] Osaki, Y.: 1974, *Publ. Astron. Soc. Jpn.* 26, 429.
- [11] Kato, S.: 1978, *Mon. Not. R. Astron. Soc.* 185, 629.
- [12] Kato, S., Honma, F. and Matsumoto, R.: 1988, *Mon. Not. R. Astron. Soc.* 231, 37.
- [13] Abramowicz, M.A., Kato S., 1989, *APJ* 336, 304 .
- [14] Chen, X. and Tamm, R.E.: 1993, *Astrophys. J.* 412, 254.
- [15] Wu, X.B., Yang, L.T., 1994, *Astrophys. J.* 432, 672.
- [16] Yu W.F, Yang L.T., Wu X.B., 1994, *MNRAS* 270, 131.
- [17] Galeev A., Rosnev R., vaiana G.S., 1978, *APJ* 229, 318.
- [18] Blandford R.D., payne G.G., 1982, *MNRAS* 199, 883.
- [19] Yang Z.L., Yang L.T., 1991, *Astron. Astrophys i.* 252, 10.
- [20] Abramowicz, M.A., Czerny, B., Lasota, J.P. and Szuskiwicz, E.: 1988, *Astrophys. J.* 332, 646.
- [21] Balbue S.A., Hawley J.F., 1991, *APJ* 376, 214.

- [22] Jones D.I. and Andersson N., Gravitational Wave Damping of Neutron Star, *Astrophys. Journ.*(2001).
- [23] Smarr L. L. Sources of Gravitational Radiation, Cambridge University Press,(1979) .
- [24] Manchester R. N. and Taylor J. H. Pulsars, San Francisco, (1977).
- [25] Timmes et al., *The Astrophysical Journal*, D457, 834,(1996).
- [26] Weber J. General Relativity and Gravitational Waves, Interscience, New York, 1, (2004).
- [27] Alder R., Bazin M., Schifter M., Introduction to General Relativity, Mc.Graw Hill,(1965).
- [28] Malcolm S.Longair, *High energy Astrophysics*,second Edition(page 133- 134),134)
- [29] Robert Popham and Rashid Sunyaev, arxiv:astro-ph/0004017 v1 (2000).
- [30] Huguenin, G. R.; Taylor, J. H.; Troland, T. H. ,*Pulsars Speed*,2007.
- [31] Juho Schult,*Studies of Accretion Disks in X-ray Binaries* (2005)
- .
- [32] F.Nagase,*J.Astrophys.Astr.*,23,59-65, (2002)
- [33] C.F.von Weizacker:*Z.Naturforsch.* 3a,524 (1948).
- [34] R.Lust:*Z.Naturforsch.*7a,87 (1952).
- [35] R.Hoshi: *Suppl.Progr.Theor.phys.*70,181 (1981).
- [36] N.Straumann:*Helv.Phys.Acta* 49,269 (1976).

Declaration

This thesis is my original work, has not been presented for a degree in any other University and that all the sources of material used for the thesis have been dully acknowledged.

Name: Haftamu G/mariam

Signature:— — — — — — — — — —

Place and time of submission: Addis Ababa University, June 2011

This thesis has been submitted for examination with my approval as University advisor.

Name: Dr.Legesse Wetro

Signature:— — — — — — — — — —